CONCENTRATION OF ELEMENTS IN MITOTIC CHROMATIN AS MEASURED BY X-RAY MICROANALYSIS

I. L. CAMERON, R. L. SPARKS, K. L. HORN, and N. R. SMITH

From the Department of Anatomy, The University of Texas Health Science Center at San Antonio, San Antonio, Texas 78284

ABSTRACT

Unfixed frozen-dried and uncoated tissue sections of the mouse duodenum were placed on carbon planchets and analyzed in a scanning electron microscope fitted with energy dispersive X-ray equipment. Computer analysis of the X-ray spectra allowed elemental microanalysis of the nucleus, cytoplasm, and mitotic chromatin regions in the cryptal and villus enterocytes. The peak to continuum ratio of S, Cl, K, and Ca were higher in mitotic chromatin than any of the other sites measured. The redistribution of Ca at mitosis is postulated to help explain both chromosome condensation and assembly of the mitotic spindle apparatus.

Knowledge of the concentration of elements at a subcellular level will increase our understanding of the mechanisms which control various cellular processes. For example, a shift in the concentration of elements may be associated with specific cellular functions such as chromatin condensation, mitosis, protoplasmic movement, cell secretion, etc.

As enough information becomes available on elemental distributions associated with the various cellular processes it seems likely that universal patterns, principles, and testable predictions will soon follow.

Ideally, measurements on elements should be made on cells or tissues which are as close to their natural or living state as possible. The current report employs unfixed frozen-dried tissue sections prepared by the method of Stumpf and Roth (10, 11). This procedure permits the localization and the measurement of diffusible and of nondiffusible tissue substances without major displacements. Briefly, the frozen-dried and uncoated sections are placed on carbon planchets and analyzed in a scanning electron microscope fitted with energy dispersive X-ray analytical equipment. The image from secondary electrons gives good enough morphological detail to identify various cellular structures and to localize areas of interest for microbeam analysis. Computer analysis of the X-ray spectra, using mineral reference standards and newly developed software programs, is used in the elemental microanalysis.

The concentrations of P, S, Cl, K, and Ca are reported as peak to continuum ratios in the nucleus and cytoplasm of duodenal crypt and villus enterocytes and in the cytoplasm and the mitotic figures of dividing crypt enterocytes. The peak to continuum ratios permits comparisons of relative concentrations of elements as related to mass of the tissue specimen (5). The ratios of four of the five elements measured were significantly higher in mitotic chromatin than any of the other sites measured.

MATERIALS AND METHODS

Pieces of duodenum about 2 mm^2 were removed from a region 1 cm below the pylorus valve of the stomach from a 20-week-old adult male C57/B1 mouse. One transversely cut surface was attached to a small tubular brass tissue-holder (2 cm long by 0.2 cm diameter), using finely minced liver as an adhesive. The tissue-holder and piece of duodenum were then rapidly frozen by immer-

sion in liquid propane cooled in a liquid nitrogen bath. The elapsed time from killing of the mouse to freezing in the propane was 45 s. The frozen tissue was then stored in liquid nitrogen until used. The tissue-holder with duodenum was removed from the liquid nitrogen and placed in a cryostat (Harris Mfg. Co., North Billerica, Mass.) at −30°C. Sections 4 μm thick were made with microtome (Damon/IEC Div., Damon Corp., Needhan Heights, Mass.) and were frozen-dried by cryosorption at −68°C for 24 h. The frozen-dried sections were then allowed to warm to room temperature before allowing air, passed through a drying agent (soda-lime), to enter the freeze-drying chamber. The tissue was then stored in a vacuum desiccator which contained calcium sulfate.

The flattest frozen-dried sections were then placed on polished, 1 inch diameter, spectrographically pure carbon planchets for SEM and X-ray analysis. No adhesives or coatings were used on the sections.

The tissue sections were then examined in a JEOL JSM-35 scanning electron microscope. The X-ray analysis system consisted of a high-angle (40°) Nuclear Semiconductor Si(Li) detector (Nuclear Semiconductor Div., United Scientific Corp., Mountainview, Calif.), and a Tracor Northern (Middleton, Wisc.) NS-880 pulse height analysis system. The active area of the detector crystal was 30 mm^2, and its resolution was 165 eV. The detector was positioned 20 mm from the specimen, which was maintained in the horizontal position at a working distance of 39 mm. Accelerating voltage was 25 kV, and a typical value of specimen current was 4×10^{-11} amperes.

Morphological information on the specimen was derived from the SEM image and was recorded photographically from the CRT on Polaroid PN-55 film. The morphology was good enough for the localization and analysis of areas of interest in the duodenal sections.

The pulse height distribution of X-rays in the range of 0–10 keV was measured by acquiring counts for 60 s (live time). Energy calibration of the pulse height analyzer was 20 eV per channel. All spectra were stored on cassette tape for later processing. The average count rate was monitored during each acquisition. A raster equivalent to 1 μm^2 was used to scan an area of the cytoplasm, the nucleus, or in the case of mitotic cells, the metaphase or anaphase chromatin or the area adjacent to the condensed chromatin and the planchet at a magnification of × 90,000.

For elemental analysis, five areas of each of the following morphological structures were analyzed: an area of the nucleus alternated with an area of the cytoplasm of interphase cells in the duodenal crypts; an area of the metaphase or anaphase chromatin alternated with an area of the cytoplasm in dividing cells; and an area of the nucleus alternated with an area of the cytoplasm of epithelial cells or enterocytes on the duodenal villi. The data were recorded and paired as nuclear or mitotic chromatin vs. cytoplasm data on each cell. In addition, five areas over the carbon planchet were measured and recorded. To test for mass or element loss or decay with elapsed time under the electron beam, spectra were acquired from an area over the cytoplasm of a villus enterocyte at times 0, 5, 10, and 15 min of continuous beam scanning at × 90,000. The specimen did not noticeably move during the test. Elemental reference spectra were recorded for $CaSO_4 \cdot 2H_2O$ (gypsum, specifically selenite); $Ca_3(PO_4)_2 \cdot CaF_2$ (fluoroapatite); NaCl (halite); KCl (sylvite); and $CaCO_3$ (Icelandic feldspar). The mineral standards were used as sources of elemental spectral structure for fitting by the Flextran Super ML (multiple least-squares) fitted algorithm program. The program accomplished quantitation of data as well as deconvolution of overlapping peaks (e.g., potassium Kβ and calcium Kα).

Analysis of elemental or continuum decay with time in a specimen was performed on peak to continuum ratios of each element and on the continuum itself by least-squares linear regression followed by comparison to a slope of zero using Student's t test.

In several cases, ratio data for individual elements in a nucleus and the cytoplasm of the same cell were analyzed as pairs by binomial expectancy statistics.

RESULTS

Figs. 1 and 2 show scanning electron micrographs of 4-μm thick frozen-dried sections of mouse duodenum photographed under conditions used for X-ray microprobe measurements. Nuclei, nuclear envelopes, mitotic chromatin, cytoplasm, and cell boundaries are all visible. The granularity or mottling seen both in the nucleus and in the cytoplasm is attributed to ice crystal damage. The continuity of the nuclear envelope indicates that tissue processing does not grossly disrupt the compartmental boundary between the nucleus and the cytoplasm. Clearly, the morphology of the tissue is adequate for the localization of discrete areas for X-ray analysis.

Fig. 3 (top) shows representative X-ray spectra

FIGURES 1 and 2 Scanning electron micrographs of frozen-dried mouse duodenum (uncoated). Figure 1. Villus—Enterocyte with nucleus (N) and nuclear envelope (NE) visible. X-ray analysis was done on a nucleus and adjacent cytoplasm. × 1920. Figure 2. Crypt—Section showing interphase and mitotic cells, nuclei, nuclear evelopes, and lumen (L) are visible. The mitotic chromatin (MC) is cross sectioned through the arms of the chromosomes. × 4160.

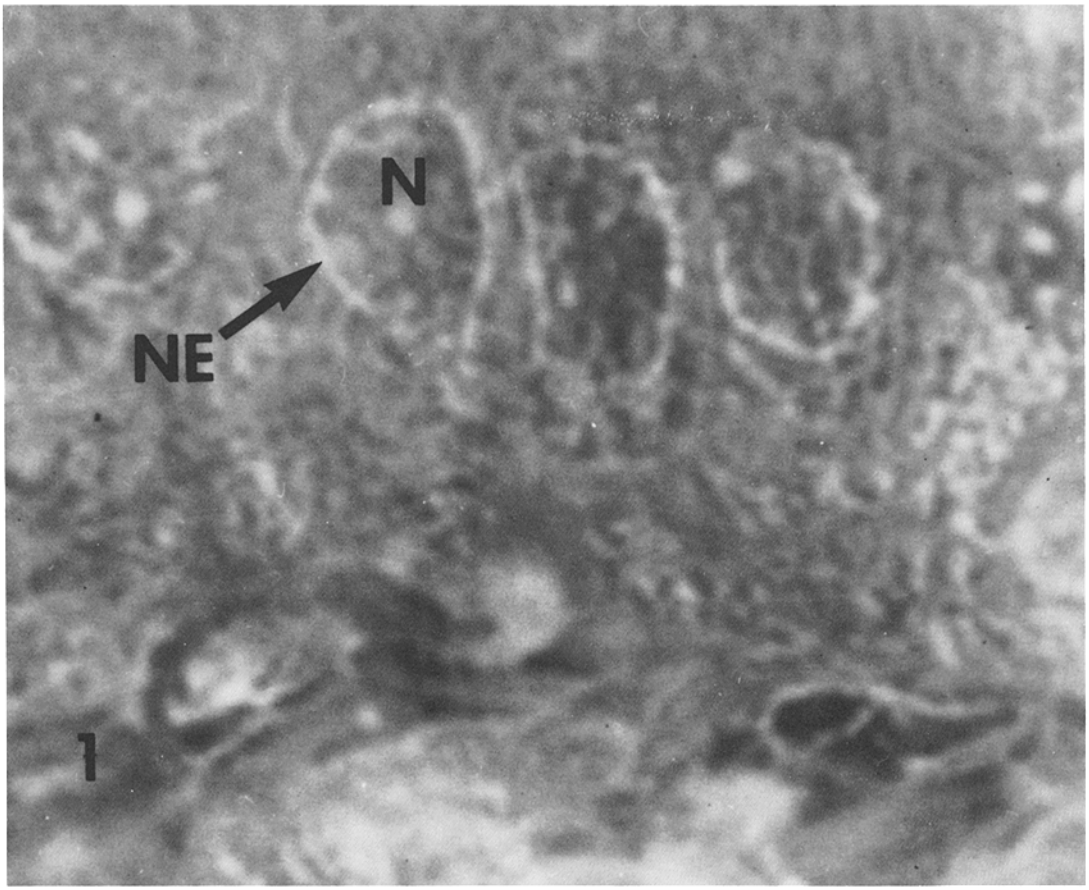
N
NE
1

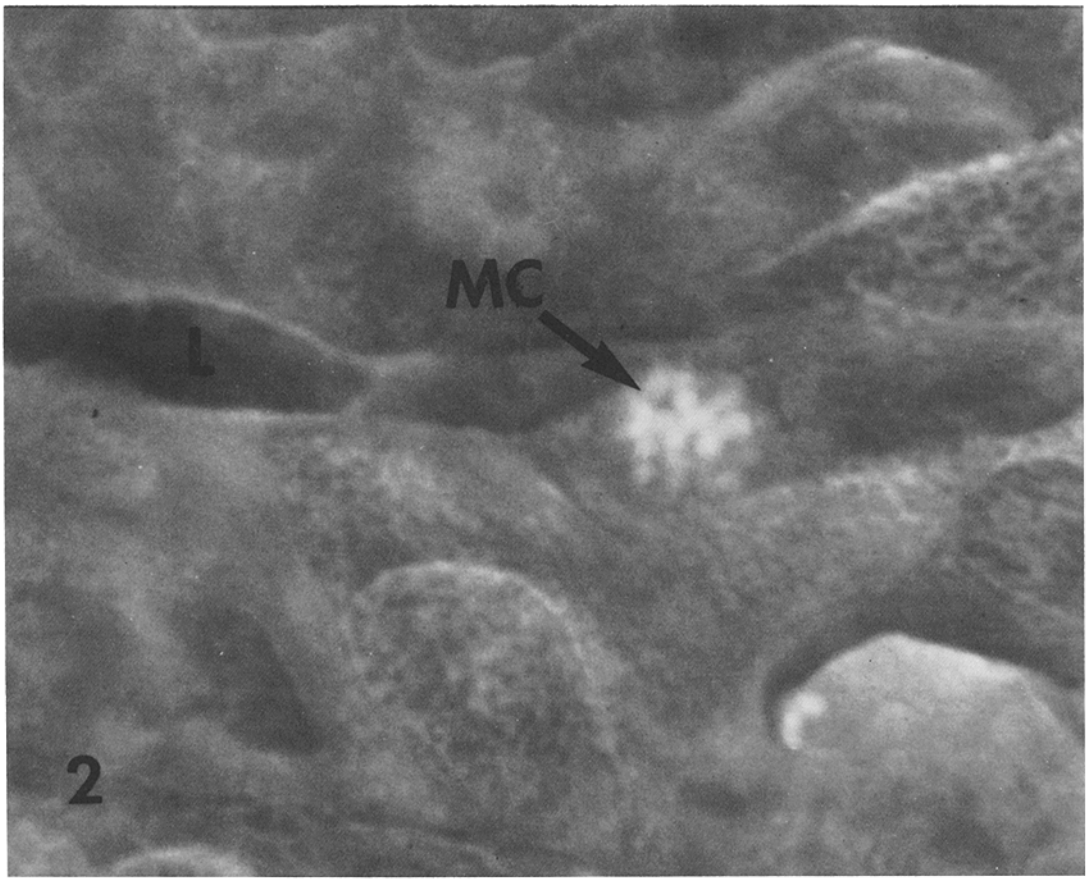
MC
L
2

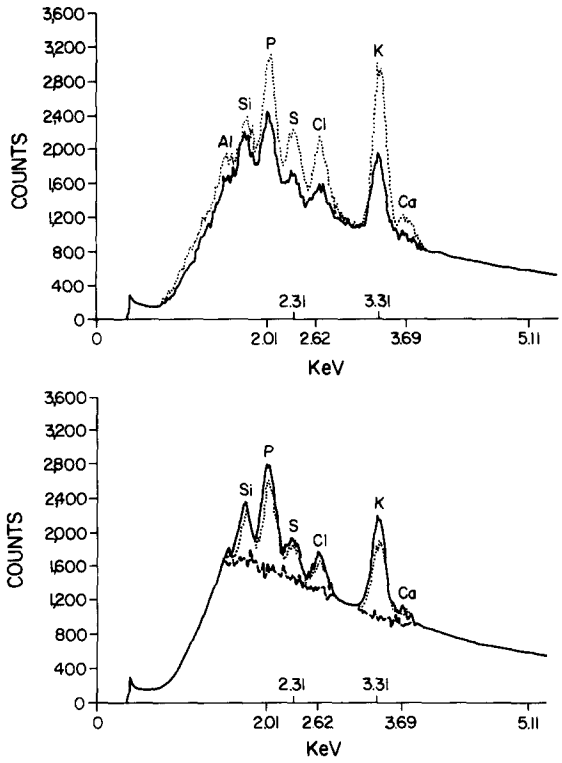

FIGURE 3 X-ray spectra of mouse duodenum. Top—Superimposed spectra of mitotic chromatin (dotted line) and adjacent cytoplasm (solid line). Note that higher counts for the labeled peaks are found in the mitotic chromatin as compared to its cytoplasm. Bottom—Superimposed spectra of an interphase nucleus (dotted line) and cytoplasm (solid line). Also, a spectrum for the carbon planchet (dashed line) used for mounting is superimposed. Note that the cytoplasm has higher peaks than the nucleus (chromatin). This is in contrast to the mitotic cell which has higher counts in the chromatin in comparison to its cytoplasm.

recorded from the cellular area of mitotic chromatin (dotted line) and from an area of the cytoplasm of the same cell (solid line). Notice that the Kα peaks for the elements P, S, Cl, and K are higher for the condensed mitotic chromatin than for the cytoplasm. The unresolved potassium Kβ-calcium Kα is also higher in the mitotic chromatin. The Bremsstrahlung ("white") or continuum radiation of both the mitotic chromatin and the cytoplasmic area appears the same in the energy range to the right of the element peaks. Fig. 3 (bottom) shows spectra from the nucleus of a cryptal cell (dotted line), from the cytoplasm (solid line) and from the carbon planchet (dashed, lower line) used to support the frozen-dried tissue section. There appears to be no great difference in the elemental concentration between the cytoplasm and nuclear area measured; however, the P, Cl, and K peaks seem somewhat greater for cytoplasm.

Table I summarizes the elemental ratios of Kα characteristic X-rays (peak minus background) to continuum for the different subcellular areas in specific states of the duodenal epithelial cell life cycle. The spectral region from 4.26 to 5.14 keV was selected for continuum measurement.

A one-way analysis of variance of the data for each element in each subcellular area shows that S, Cl, K, and Ca are significantly higher over the metaphase-anaphase chromatin of cryptal cells than any other area measured ($p < 0.001$). The variability in the ratios of P, especially for the

TABLE I

Elemental Ratios (Mean ± SEM) of Kα Characteristic X-rays (Peak Minus Background) to Continuum for Analyzed Areas of Duodenal Cells in Frozen-Dried Tissue Sections*

	A	B	ratio A/B
	Interphase nucleus of crypt cell	Interphase cytoplasm of crypt cell	
Phosphorus	.369 ± .0072	.410 ± .0069	.900
Chlorine	.119 ± .0086	.157 ± .0102	.758
Potassium	.339 ± .0078	.401 ± .0050	.845
Sulfur	.131 ± .0074	.139 ± .0098	.942
Calcium	.015 ± .0033	.022 ± .0217	.682
Continuum§	20.22 ± .204	20.31 ± .178	0.996
	Mitotic chromatin of crypt cell	Cytoplasm of mitotic crypt cell	
Phosphorus	.300 ± .0895	.341 ± .0239	.880
Chlorine	.369 ± .0442‡	.146 ± .0165	2.527
Potassium	.662 ± .0745‡	.375 ± .0263	1.765
Sulfur	.429 ± .0757‡	.159 ± .0226	2.698
Calcium	.083 ± .0125‡	.022 ± .0130	3.773
Continuum	21.58 ± 1.769	21.10 ± 1.524	1.023
	Nucleus of villus cell	Cytoplasm of villus cell	
Phosphorus	.359 ± .0087	.387 ± .0314	.927
Chlorine	.131 ± .0040	.156 ± .0041	.840
Potassium	.336 ± .0177	.397 ± .0153	.846
Sulfur	.136 ± .0072	.151 ± .0066	.900
Calcium	.019 ± .0125	.017 ± .0070	1.117
Continuum	21.73 ± .060	21.54 ± .044	1.009

* Mean is from 5 areas over 5 different cells

‡ One-way analysis of variance of all data for each element plus calculations of standard errors of differences between means using Student's t values show these elements to be higher in concentration ($p < 0.001$) than any others. No other means are significantly different.

§ Continuum is determined from total X-ray counts (times 10^3) generated from the Bremsstrahlung continuum (4.26–5.14keV).

metaphase-anaphase chromatin area, was larger than any other set of elemental values over any other area. The reason for such variability is not clear. No other significant differences were found in the mean value comparisons as subjected to Student's t test analysis.

Although no other set of mean values is significantly different, an analysis of paired data of the elements between the nucleus and the cytoplasm of the five cryptal and the five villus cells shows the P, S, Cl, and K to be higher in the cytoplasm in all cases, except P in the villus cells and S in the cryptal cells. With these two specific exceptions, the elemental concentration in the cytoplasm is significantly higher according to binomial expectancy analysis ($p < 0.05$).

Elemental concentration of peaks over a specific area of the cytoplasm of one cell was measured at 0, 5, 10 and 15 min under the X-ray conditions used above. This time study was deemed necessary in light of reports of beam-induced loss in organic specimens (6). The values of peak to continuum ratios were subjected to least squares linear regression analysis and gave the following values: P, slope 0.003, correlation coefficient (r) 0.595; S, slope 0.001, r 0.774; Cl, slope 0.002, r 0.745; K, slope 0.003, r 0.996; Ca, slope −0.00007, r 0.999; and continuum counts, slope −0.14, r 0.085. No slope gave a value significantly different than a slope of zero value, nor were any of the slopes substantially negative. From this, it appears that there was no significant loss of elements or continuum counts with continuous beam exposure under the conditions used in this study, at least from the time the readings were begun.

DISCUSSION

The frozen sections used in this study are not meant to reveal optimal morphological detail but are meant to provide new information on the elemental concentration of cell organelles in tissue prepared for X-ray analysis by procedures which spatially retain the elements in as close to the natural living state as possible. Stumpf and Roth (10, 11) and Brown et al. (4) have developed and rigorously tested the same frozen-dried section preparative procedure we have used and find that movement of soluble diffusible substances is prevented. Assurance can therefore be given that we are examining cells and tissues which have undergone no major translocation of elements. As an example of the resolution and usefulness of this procedure, Brown et al. (4) have shown that three water-soluble radioactively labeled extracellular space indicators were maintained in the extracellular space, using dry mounting radioautographic techniques. Nevertheless, before proceeding with discussion of the distribution of elements as seen in our study, it seems worthwhile to mention possible technical problems which may influence element distribution. Bacaner et al. (3) have indicated that some redistribution of elements can occur if the tissues are not frozen at a fast enough rate. The faster the freezing rate, the smaller the ice crystals. During ice crystal formation, the elements are preferentially distributed to the ice crystal boundary. This presents more of a problem when dealing with element distribution interpretation at the ultrastructure level than it does with the lower magnification level used in the present study.

The ice crystal damage visible in Fig. 1 is certainly responsible for some redistribution of elements, at least to the extent of the dimensions of the ice crystals. Hodson and Williams (7) have shown that frozen-dried sections can quickly rehydrate, which can reseal ice crystal damage so that the damage is no longer apparent. Such rehydration could also lead to element diffusion. Our sections were dehydrated and brought to room temperature under vacuum to minimize rehydration and the resealing of ice crystal damage. Thus, we feel safe in saying that no major translocation of elements has occurred at the level of structures at which we are working. We would have to be more cautious if we were working at an ultrastructural level.

Frozen sections in the hydrated state are even closer to the natural or living state than frozen-dried sections; however, the methods and equipment used are only just beginning to be developed and tested (9).

There are little data available in the literature with which to compare our elemental distribution and concentration data. Both our data and those of Appleton (1, 2) show that element peak to continuum ratios for potassium are higher in ground cytoplasm than in the nucleus.

Although no data on elemental distribution in mitotic chromatin could be found in the literature, Weaver (12) has reported an increased peak to continuum ratio of calcium in condensed nuclear chromatin areas as compared to uncondensed nuclear chromatin areas in the nucleus of pancreatic acinar cells. This finding agrees with our finding of

an increase in calcium in condensed mitotic chromatin vs. chromatin in the interphase nucleus.

In conflict with our report, Saubermann and Echlin (9) reported that K, S, and Cl give higher element peak to continuum ratios in nuclear areas as compared to cytoplasmic areas of hepatocytes; however, only Cl was reported to be significantly higher in the nuclear area. Their reported results were similar when sections were analyzed in the frozen-hydrated or the frozen-dried state. Just why our results should show the opposite concentration of these elements between the nucleus and the cytoplasm is not entirely clear. Perhaps our sample size was larger or there was some difference in sample area measured, or perhaps our more refined computational systems and software programs permit a more definitive analysis.

The elemental concentrations of P, Cl, K, S, and Ca are generally lower in the nucleus than the cytoplasm in interphase (cryptal) and postmitotic (villus) enterocytes. This is reflected in a nucleus to cytoplasmic concentration ratio of less than one (column to the far right in Table I). This difference between the nucleus and cytoplasm must be related to the nuclear-cytoplasmic compartmentalization and may have as its basis the intact nuclear envelope. At mitosis when the nuclear envelope is known to disintegrate, there is a significant concentration of Cl, K, S, and Ca in the mitotic chromatin. A concentration of elements in chromosomes could most simply be explained by a closer packing of elements into a smaller space; however, such a simple explanation might be expected to bring about a uniform concentration of the various elements and lead to a rather constant packing or concentration ratio for each element. In fact, the concentration ratios of elements in mitotic chromatin vs. the cytoplasm have a rather wide range of values. This difference in element concentration in mitotic chromatin suggests that some elements are preferentially redistributed during chromosome condensation. Ca appears to be concentrated in condensed chromatin to a greater extent than the other elements. It seems worthwhile to speculate on the meaning of this observation in relation to chromosome condensation and to formation of the mitotic spindle apparatus. Some observations of Mazia (8) help us explain how Ca redistribution might function in mitosis. He points out that assembly of microtubules into spindle fibers may be caused by a lowering of the free Ca concentration. The sequestering of the free Ca by condensing chromosomes is suggested by our findings. We speculate that the sequestering of free Ca by chromosomes might result in a lower free Ca concentration which may be associated with assembly of mitotubules into a mitotic spindle apparatus. Experience and the literature also suggest that chromatin condensation may be caused by calcium and other divalent cations (8). Thus, the concentration of calcium by condensing chromatin may help explain both chromosome condensation and the assembly of the mitotic spindle apparatus during mitosis.

This work was supported by U. S. Public Health Services grant CA16831 from The National Cancer Institute.

Received for publication 30 August 1976, and in revised form 16 December 1976

REFERENCES

1. Appleton, T. C. 1972. "Dry" frozen sections of unfixed and unembedded biological material for x-ray microanalysis of naturally occurring diffusible electrolytes: the cryostat approach. *J. Microsc. (Paris).* **13:**144–147.
2. Appleton, T. C. 1974. A cryostat approach to ultrathin 'dry' frozen sections for electron microscopy: a morphological and x-ray analytical study. *J. Microsc. (Oxf.).* **100:**49–74.
3. Bacaner, M., J. Broadhurst, T. Hutchinson, and J. Lilley. 1973. Scanning transmission electron microscope studies of deep-frozen unfixed muscle correlated with spatial localization of intracellular elements by fluorescent x-ray analysis. *Proc. Natl. Acad. Sci. U. S. A.* **70:**3423–3427.
4. Brown, D. A., W. E. Stumpf, and L. J. Roth. 1969. Localization of radioactive labelled extracellular fluid indicators in nervous tissue by autoradiography. *J. Cell Sci.* **4:**265–288.
5. Hall, T. A., C. H. Anderson, and T. Appleton. 1973. The use of thin specimens for x-ray microanalysis in biology. *J. Microsc. (Oxf.).* **99:**177–182.
6. Hall, T. A., and B. L. Gupta. 1974. Beam-induced loss of organic mass under electron microprobe conditions. J. Microsc. (*Oxf.*). **100:**177.
7. Hodson, S., and L. Williams. 1976. Ultramicrotomy of biological tissues to preserve membrane structure. *J. Cell Sci.* **20:**687–698.
8. Mazia, D. 1974. The chromosome cycle in the cell cycle. *In* Cell Cycle Controls. G. M. Padilla, I. L. Cameron, and A. M. Zimmerman, editors. Academic Press Inc., New York. 265–272.
9. Saubermann, A. J., and P. Echlin. 1975. The preparation, examination and analysis of frozen hydrated tissue sections by scanning transmission electron microscopy and x-ray microanalysis. *J. Microsc. (Oxf.).* **105:**155–191.

10. STUMPF, W. E., and L. J. ROTH. 1962. High resolution autoradiography with dry-mounting, freeze-dried frozen sections. *J. Histochem. Cytochem.* **14:**274–287.
11. STUMPF, W. E., and L. J. ROTH. 1969. Autoradiography using dry-mounted freeze-dried sections. *In* Autoradiography of Diffusible Substances. L. J. Roth and W. E. Stumpf, editors. Academic Press Inc., New York. 69–80.
12. WEAVER, B. A. 1973. Combined transmission electron microscopy and x-ray microanalysis of ultrathin frozen dried sections-an investigation to determine the normal elemental composition of mammalian tissue. *J. Microsc. (Oxf.).* **97:**331–341.